Heliyon 7 (2021) e06065

Contents lists available at ScienceDirect

Heliyon

journal homepage: www.cell.com/heliyon

Research article

Experimental and DFT calculation study of interaction between silver nanoparticle and 1-butyl-3-methyl imidazolium tetrafluoroborate ionic liquid

Madhulata Shukla [a,*], Alkadevi Verma [b], Sunil Kumar [c], Shaili Pal [c], Indrajit Sinha [c,**]

[a] Department of Chemistry, G.B. College, Veer Kunwar Singh University, Ramgarh, Kaimur, Bihar, India
[b] Department of Chemistry, Rewa Engineering College, Rewa 486002, Madhya Pradesh, India
[c] Department of Chemistry, Indian Institute of Technology (Banaras Hindu University), Varanasi 221005, India

ARTICLE INFO

Keywords:
Green synthesis
Nanoparticle stabilization
Ionic liquids
DFT calculation
Charge distribution

ABSTRACT

The mechanism of stabilization of silver nanoparticles (Ag NPs) by 1-butyl-3-methylimidazolium tetrafluoroborate ionic liquid (IL) is elucidated from experimental spectroscopic investigations and density functional theory (DFT) calculations. FTIR spectrum of the synthesized IL stabilized silver nanoparticles reveals small red shift in B–F stretching frequency while C–H stretching remains unshifted. There is no shift in NMR peaks of IL before and after the synthesis of IL stabilized Ag NPs. This suggests that Ag NPs are surrounded by anions of ILs. The optimized structure obtained from density functional theory (DFT) calculations also shows the anionic part of the IL surrounding the Ag nanocluster. This is supported by the IR frequency data calculated using DFT. The calculated binding energy and interaction energy obtained between cluster and IL is considerably attractive. Density of State (DOS) calculation shows that the HOMO-LUMO gap of the Ag cluster-IL composite is significantly lesser than that of the IL alone.

1. Introduction

Ionic liquids (ILs) act as electronic as well as steric stabilizers preventing nanoparticle (NP) growth and nanoparticle aggregation. Synthesis conditions with high reaction and nucleation rates can be achieved leading to the formation of extremely small nanoparticles [1, 2].Being new materials, the catalytic properties of such nanocomposites are being extensively studied currently. Nevertheless, only a few research papers have investigated the effect of such stabilization of nanoparticle surfaces on the electronic properties of such nanocomposites [3]. Moreover, limited studies have taken up the issue of effect of IL stabilization on the catalytic properties of these particles. This becomes topical in view of the fact that a few recent experimental as well as theoretical investigations have shown that many macromolecules (other than ILs) stabilizing nanoparticles also affect their electronic structures and thereby their catalytic activity [4, 5, 6]. Imidazolium based ionic liquids have highly structural organization at nanoscale level and in the condensed phase [7], containing supramolecular networks held together by hydrogen bonds and π−π stacking between imidazolium rings [8, 9] Synthesis, interaction and organization of NPs in ILs have been explained deeply by He et.al [10]. In this report, stability of nanoparticle dispersions in ionic liquids and the intermolecular forces affecting its stability has been well explained. Imidazolium based ionic liquids with stable anions e.g., tetrafluoroborate are the best materials for synthesis of NPs because of its stability and basic properties of the bmimBF4 [11]. Many reports are available explaining the synthesis of different NPs in ILs containing BF4 anion [6, 12, 13] NP shape and size vary deeply with the amount of IL used, type of IL used as well as trace amount of impurities and water present in ILs [6, 13].

DFT calculations can be employed to understand such mechanistic issues and to analyse the effect of ILs on the NPs. Abroshan et.al reported molecular level understanding of oxidative addition of Au25(SCH3)18 to a halide in ILs using DFT calculations with B3PW91 hybrid density functional and 6-31G(d,p) and LANL2DZ basis sets [14].

Few reports are available for the synthesis of Ag in 1-butyl-3-methyl imidazolium based ILs [6, 15]. The present paper first reports the synthesis of Ag NPs stabilized by 1-butyl-3-methylimidazolium tetrafluoroborate (bmimBF4) IL with glucose as the reducing agent. We then

* Corresponding author.
** Corresponding author.
E-mail addresses: madhu1.shukla@gmail.com (M. Shukla), isinha.apc@iitbhu.ac.in (I. Sinha).

https://doi.org/10.1016/j.heliyon.2021.e06065
Received 4 August 2020; Received in revised form 12 October 2020; Accepted 19 January 2021

investigate orientation and interaction of cation and anion parts of IL around the nanocluster, experimentally using NMR and IR spectroscopy. DFT calculations are performed to analyze whether IL just acts as a stabilizer to prevent the aggregation of NPs clusters or also act as an electron donor to activate the Ag clusters for further reaction. The change in HOMO and LUMO energy gap that occurs when IL stabilizes the Ag cluster is compared to the HOMO-LUMO gap of the pure IL. Results from spectroscopic investigations are found to be in agreement with those obtained from DFT calculations. Literature survey shows that B3LYP functional calculations give the stable cluster and also reproduce the experimental results [16, 17, 18] Very recently we have shown in our previous research that B3LYP functional calculations give the stable nanocluster and also reproduce well with the experimental results obtained for UV visible and IR spectra [19, 20].

2. Methodology

2.1. Synthesis and characterization of Ag NP in bmimBF4 IL

Materials used for synthesis of silver nanoparticles were $AgNO_3$ (Merck), $bmimBF_4$ (IoliTech), glucose (Merck). All reagents were used as received without further purification. 2 mL aqueous 0.05 M $AgNO_3$ solution was taken in a round bottom flask. This flask was then kept in a preheated water bath maintained at 80 °C. To this flask, of 2 mL of 0.1 M aqueous glucose solution was added in drop wise manner with continuous stirring. Stirring was continued for 15 min at 80 °C. The UV-visible spectrum of the resultant solution was then recorded. Two peaks were observed, one at 300 nm and another at 430 nm (quite broad peak). Afterwards 2 mL bmimBF4 IL was added drop wise to the above reaction mixture with continuous stirring for further 30 min at 105–110 °C in oil bath to remove almost all the waters present in the solution. Again UV-visible spectra was recorded, the peaks remain unchanged. Continuous stirring of the reaction mixture at 105 °C was continued and UV-visible spectra of the reaction mixture were recorded at every 30 min interval. Both the peaks observed in the initial UV-vis spectrum remain as such till 150 min. After completion of 3 h, UV-visible spectra (Figure 1) shows a peak shift from 430 nm (broad) to 423 nm (quite sharp), which suggests the formation of silver NP (AgNPs). AgNPs solution was light yellow in colour. Further sample characterization was done by FTIR, NMR and TEM.

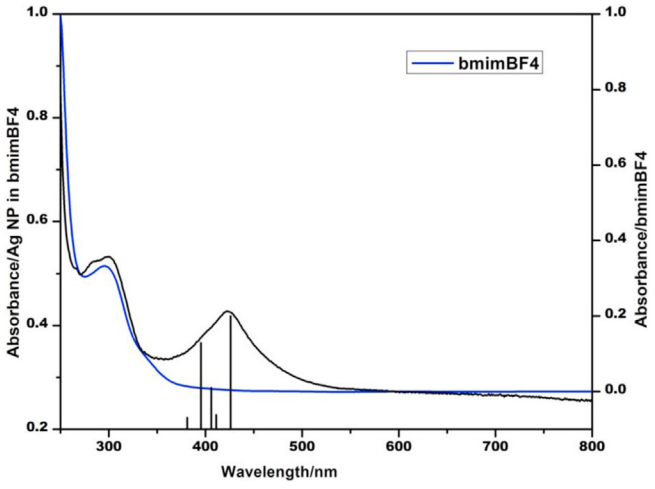

Figure 1. UV-visible spectrum of Ag-NP in bmimBF4 IL using Glucose as reducing agent (black line) (Peak at 423 nm confirms the formation of silver nanoparticles). Blue colour line represents UV-visible spectrum of neat bmimBF4 IL. Vertical black colour line represents the TD-DFT calculation of Ag-bmimBF4 cluster. Transitions of our interest only has been shown in the figure to avoid confusion.

2.2. Characterization

Agilent Cary 60 spectrophotometer was used to record the UV-Visible absorption spectra of IL-AgNPs dispersion inaqueous medium. X-ray diffraction measurements were carried out by Rigaku Mini-X 600, Japan. Transmission electron microscopy imaging and electron diffraction of as prepared IL AgNPs was carried out with TECNAI 20 G2-electron microscope operating at voltage of 200 kV.

2.3. Computational details

A 13 atom cluster was carved out of the FCC Ag lattice constructed using the MAPS software (Scienomics). Gaussian 16 program [21] package was employed for DFT calculations at the Becke's three parameter functional and Lee–Yang–Parr hybrid functional (B3LYP) level [22, 23] of calculation. LANL2DZ basis set was used for silver atoms [24] and 6-31G++(d,p) basis set for C, H, N, B and F atoms. Literature survey shows that B3LYP functional calculations give the stable cluster and also reproduce the experimental UV visible and IR data very well [19, 20] Two models were investigated. The first model, henceforth denoted by Ag13-1$bmimBF_4$, was one in which the interaction between 13 atom Ag cluster and only one $bmimBF_4$molecule was studied. In the second model (Ag13-2bmimBF4) the 13 atom Ag cluster was surrounded by two $bmimBF_4$(IL) molecules. Calculations were carried out for ground state geometry optimization in gaseous phase. The Natural Bonding Orbital (NBO) charges of each atom were calculated by the NBO analysis. Density of states (DOS) was calculated using GaussSum program [25] to analyse the band gap present in a molecule. IR frequency was calculated on the optimized structure using same basis set and at same level of calculation using Gaussian 16 Program. The absence of imaginary frequencies at all optimized ground states justified that the proposed geometry is a minimum and not a transition state (TS) intermediate. Binding energy (B.E.) of Ag13 and interaction energy of Ag13 cluster with two bmimBF4 moiety calculated at same level of calculation. Finally TD-DFT calculation done to obtain the energy, oscillator strength and wavelength and was correlated with the experimental UV visible spectrum.

3. Results and discussion

3.1. Spectroscopic investigations

UV-visible spectrum of the IL-AgNPs dispersion prepared by the protocol given in the section 2.1 has been shown in Figure 1. The maximum absorbance peak in the spectrum of the prepared dispersion is located at about 423 nm. This is characteristic of the localized surface plasmon resonance absorption due to AgNPs. Figure 2 displays the TEM micrograph of the prepared AgNPs sample and their corresponding electron diffraction pattern. Figure 2a shows bright field TEM image of bmimBF4 IL stabilized AgNPs. Particles with size ranging from 55 - 135 nm are observed. Anisotropic shapes such as hexagonal, pentagonal and triangular nanoparticles can be seen (shown in Figure 2a). NP shape and size vary extremely with the type and amount of IL used, as well as trace amount of impurities or water present in ILs effect its shape and size [9, 26, 27]. The electron diffraction ring pattern, shown in Figure 2b, could be indexed to FCC Ag. This confirms the formation of IL stabilized AgNPs.

To better understand the mechanism of stabilization of AgNPs by bmimBF4 IL, comparisons were made between the FTIR of the pure IL and that of IL containing AgNPs. These FTIR's are shown in Figure 3. The 850 cm^{-1} peak in pure IL shifts to 833 cm^{-1} (red shift) for AgNPs synthesized in IL. Other peak at 1062 cm^{-1} in pure IL gets red shifted to1028 cm^{-1} in Ag-bmimBF4.Obtained product was further characterized by ^{1}H(Figure S1a, b) and ^{13}C NMR spectra (Figure S2). No shift in NMR peaks could be observed when a comparison was made between the spectrums of pure IL (Figure S3a, b for ^{1}H NMR and S4a & S4b for ^{13}C NMR) and AgNPs prepared in same IL. This confirms that Ag cluster is

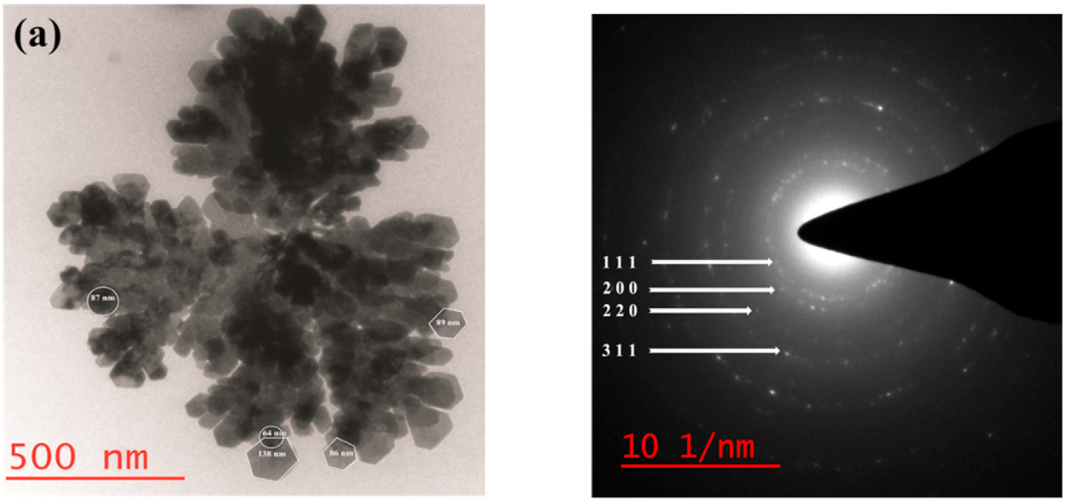

Figure 2. a) TEM image of bmimBF4 IL stabilized AgNPs, b) Selected area electron diffraction pattern.

surrounded only by anions but not by cations, as reported earlier also [28, 29].

3.2. Geometry optimization

Ag13, bmimBF4, Ag13-1bmimBF$_4$ and Ag13-2bmimBF4 moieties were optimized in gas phase at B3LYP level of calculation and using Gaussian 16 program. Figure 4(a) and (b) represents the optimized structure of Ag13-1bmimBF4 and Ag13-2bmimBF4 respectively in which several interactions are shown by the dotted line. It is clear from Figure 4 that BF4 is oriented more towards the silver cluster instead of imidazolium cation. This statement proposed earlier in literature [6, 28, 29] gets verified for the first time from our calculation. This indicates that silver nanoparticles are surrounded by more number of anions rather than cations. Also this statement has been supported by the NMR data where it was found that no NMR shift was observed for IL before the synthesis and after the synthesis (Figure S3).

To analyse the charge distribution on silver cluster and IL, Natural Bond Orbital (NBO charge) analysis of Ag13-2bmimBF4 moiety was carried out and is shown in Figure 5. Figure 5 shows that central atom of the nanocluster is quite negative (shown in red colour) while rest of the atoms are positively charged (green colour). Also it is shown that F atom of $BF4^-$ are negatively charged (red colour) and will be attracted towards the positively charged silver atoms present on outer layer of the silver cluster. Interaction energy calculated (shown in Section 3.4) for Ag13-2bmimBF4 suggests that strong interaction is present between cluster and ILs. Hence, it holds the ILs well and stabilizes the NP with strong interaction.

To better understand the changes in the electronic structure of the Ag cluster on its conjugation with the IL molecule, the change in the HOMO-LUMO gap of the pure IL on its interaction with Ag13 cluster was studied [7]. The HOMO-LUMO gap analysis was done by performing DOS calculation using Gaussum program. DOS pictures obtained for bmimBF4, Ag13-1bmimBF4 and Ag13-2bmimBF4 are shown in

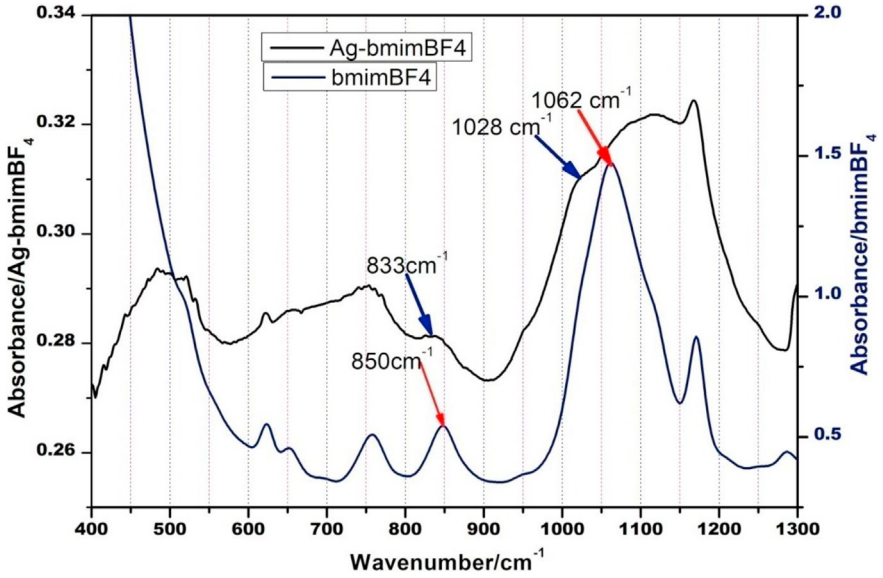

Figure 3. Experimental IR spectra of pure bmimBF4 IL and IL containing silver NPs.

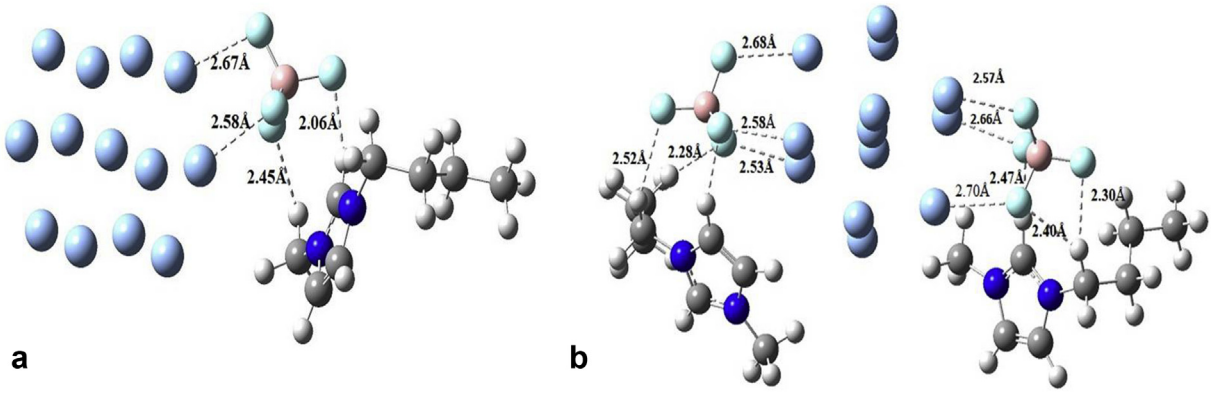

Figure 4. Optimized structure of (a) Ag13-1bmimBF4 and (b) Ag13-2bmimBF4 moiety.

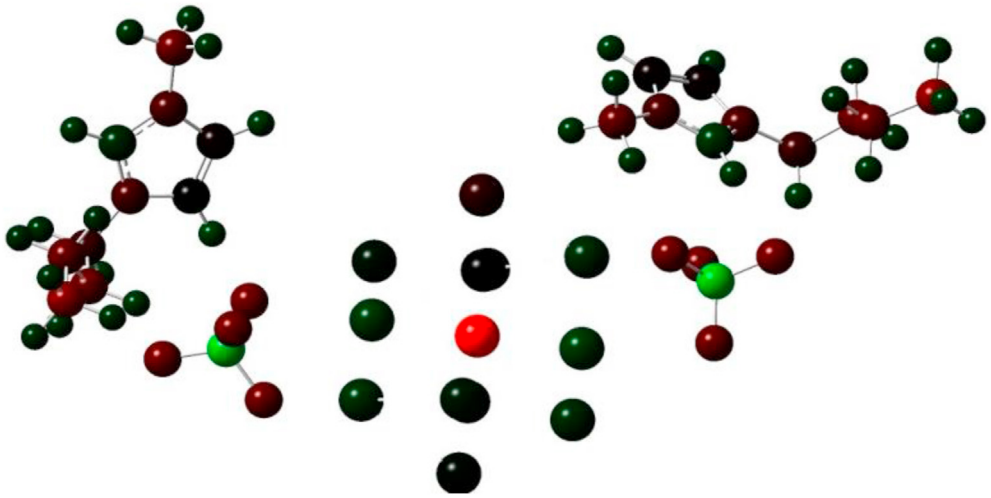

Figure 5. NBO charge distribution on Ag13-2bmimBF4 (Red colour represents the most electronegative element and green colour represents the electron deficient atom) indicating that BF4 ions are much closer to the Ag13 cluster.

Figures 6, 7 and 8 respectively. Figure 6 reveals that energy gap between HOMO and LUMO is quite high for bmimBF4 ion pair. With addition of IL to Ag13 cluster, band gap decreases hugely and DFT data (data given in Supplementary) supports this finding also. The gap decreases when the number of bmimBF4 is increased to two.

3.3. Calculated IR spectra analysis

The strength and nature of interaction between the Ag cluster and the IL molecules can be better understood through IR frequency calculations. Accordingly, IR frequency calculations were performed on the optimized structure of bmimBF4, Ag13-1bmimBF4 and Ag13-2bmimBF4 moiety at the same B3LYP level of calculation and same basis set. The calculated data is presented in Table 1. Calculated frequencies at 842 and 1075 cm^{-1}, which is due to symmetric and asymmetric stretching of B–F bond in bmimBF4 ion pair, gets red shifted to 822 and 1061 cm^{-1} respectively for Ag13-1bmimBF4. As mentioned earlier in section 3.1, the experimental FTIR spectrum shows that two peaks (at 850 and 1062 cm^{-1}) in pure IL get red-shifted in AgNPs-IL. Therefore, the calculated results are in agreement with experimental observations mentioned earlier.

Except the C2–H frequency, other calculated C–H frequencies do not show any shift. The calculated C2–H stretching present at 3273 cm^{-1} in bmimBF4 ion pair gets blue shifted to 3332 cm^{-1} in Ag13-1-bmimBF4 cluster. This indicates that the C2–H bond is affected by the IL-Ag cluster interaction. The interaction between imidazolium cation and BF4 anion is quite strong in isolated form. However, this interaction weakens when BF4 gets attached to the Ag cluster. To conclude, BF4 is more closely attached to Ag cluster. This decreases the interaction between cation and anion part of the IL. Lack of shift in other C–H stretching frequencies indicates that imidazolium ring remains unaffected. Moreover, the imidazolium ring part is located away from the Ag cluster whereas the anionic part interacts strongly with the Ag cluster.

3.4. Binding energy and interaction energy calculation

The binding energies (E_b) for A_mB_n NPs are defined by Eq. (1) [30]-

$$Eb = \{ E(A_mB_n)\text{-}mE(A)\text{-}nE(B)\}/(m + n)\text{…….. [30]} \quad (1)$$

Binding energy of Ag13 cluster calculated using DFT at B3LYP level and LanL2DZ basis set. Binding energy of Ag13 nanocluster found to be -4. 54 eV. Negative values of E_b demonstrate that the formations of Ag NPs are energetically favorable.

The interaction energy is a good aid to evaluate whether the formed interacted system is thermodynamically favorable or not. Interaction energy (I.E.) is defined as the energy difference between the optimized

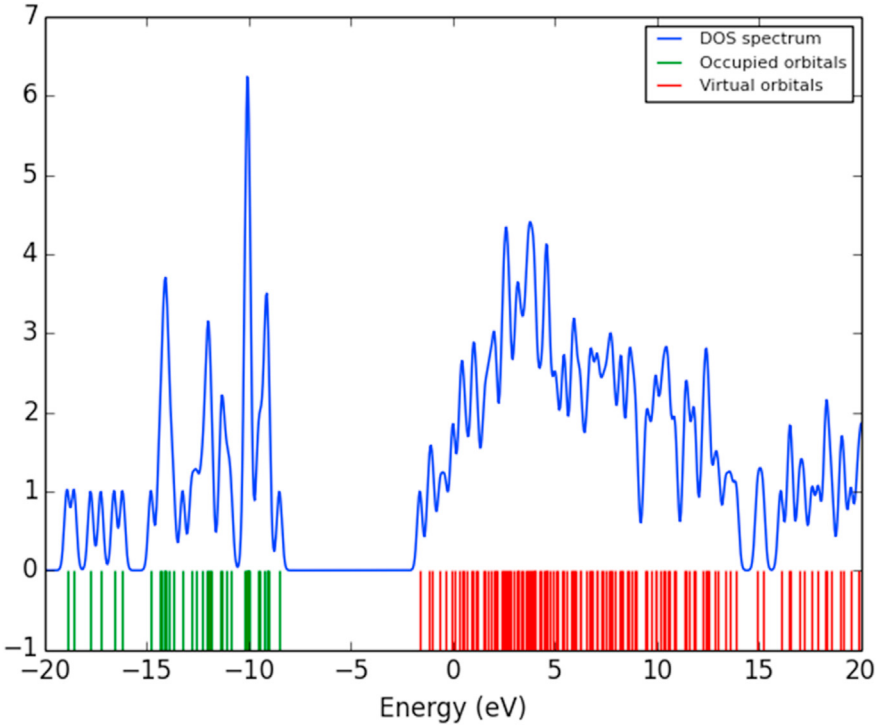

Figure 6. Density of state plot for bmimBF4 IL. Band gap (HOMO-LUMO gap) is quite large for simple IL.

structures of final (after adsorption) and initial (before adsorption) state as shown by Eq. (2) [31].

Interaction energy = Energy of Ag_{13}-2bmimBF$_4$ –[Energy of Ag13+ 2xEnergy of bmimBF4] ..... [31] (2)

Interaction energy of Ag13-2bmimBF4 moiety calculated to be -12.35eV. Higher the value of interaction energy, stronger will be the adsorption [29]. Hence higher value of interaction energy of Ag13-2bmimBF4 system is a good aid to state that interacted system is thermodynamically favourable.

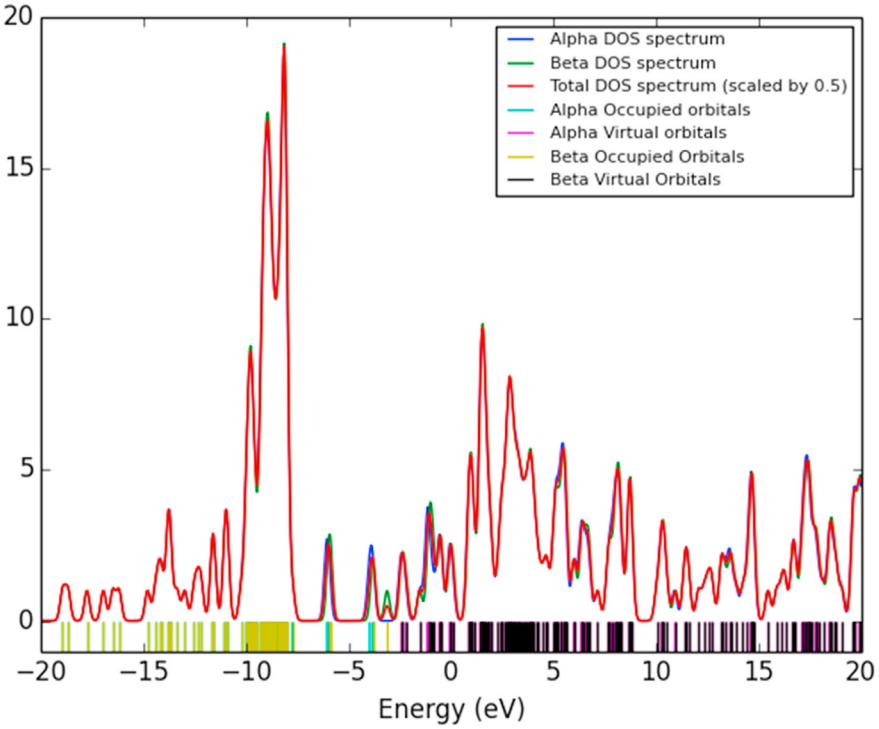

Figure 7. Density of state plot for Ag13-1bmimBF4 IL. Band gap (HOMO-LUMO gap) decreases to a large extent as compared to simple IL.

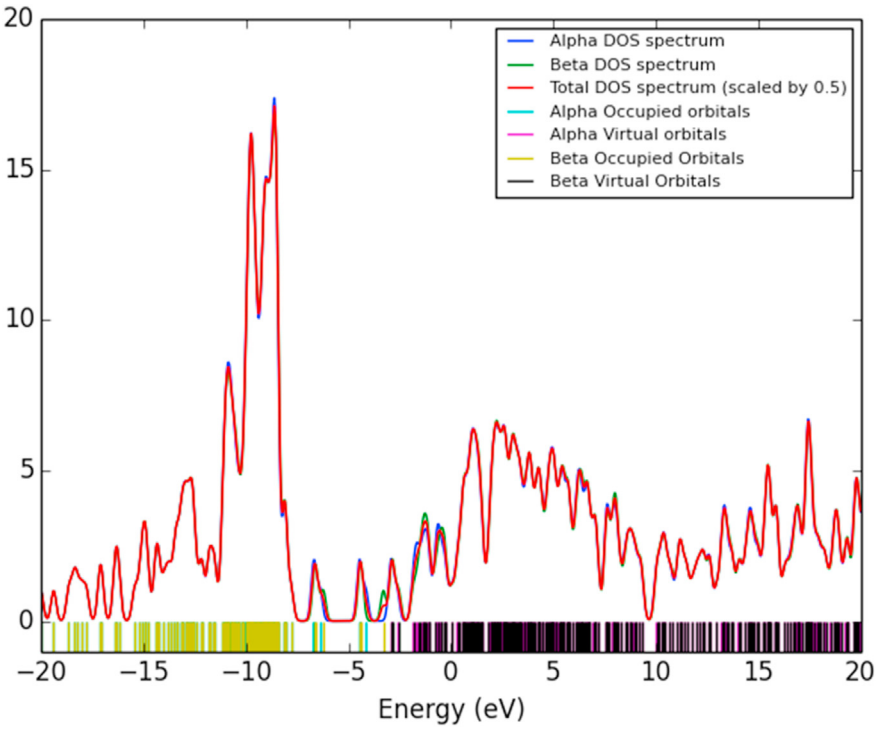

Figure 8. Density of state picture for Ag13-2bmimBF4 IL. Band gap decreases even more.

Table 1. Calculated IR frequency of bmimBF4, Ag13-1-bmimBF4 and Ag13-2-bmimBF4.

Wavenumber/cm^{-1}/bmimBF4	Wavenumber/cm^{-1}/Ag13-1-bmimBF4	Wavenumber/cm^{-1}/Ag13-2-bmimBF4	Assignment
699	692	698	Op bending of C–H in imidazole ring
842	822	7818	Symmetric stretching of B–F
932	943	953	Op bending of C2–H in imidazole ring
967	1006	1012	Op bending of C2–H in imidazole ring coupled with B–F asymmetric stretching
1016	1052	1058	Scissoring of C–N–C in imidazole ring coupled with B–F asymmetric stretching
1075	1061	1060	Asymmetric B–F stretching coupled with C–N stretching
1193	1197	1193	C2–H and C–H ip bending coupled with C–H rocking in H–C–H and C–N stretching
1469	1463	1467	Umbrella bending in CH3 gr
1523	1526	1523	H–C–H scissoring in CH3 gr
1604	1596	1596	C=N str coupled with C=C sr
3034	3042	3038	Symmetric C–H str in CH3
3069	3069	3059	Symmetric C–H str in terminal CH3 gr
3084	3082	3099	Asymmetric C–H str in CH2 gr
3112	3115	3115	Asymmetric C–H str in terminal CH3 gr
3273	3332	3322	C2–H stretching

4. Conclusions

Green synthesis of silver nanoparticles (AgNPs) stabilized by 1-butyl-3-methylimidazolium tetrafluoroborate (bmimBF4) IL has been carried out with glucose as the reducing agent. Unlike other slower green synthesis protocols, the synthesis is completed in only three hours' time. This is primarily due to the use of small amount of water as solvent in the beginning with IL molecules acting as the nanoparticle stabilizers. Anisotropic AgNPs (55–135 nm) with shapes such as hexagonal, pentagonal and triangular have been formed under these conditions. Two peaks (only of anion) of the FTIR of the pure IL undergo red-shift when the IL stabilizes AgNPs. However, the ^{1}H NMR does not exhibit any concomitant shift. This indicates that the IL molecules stabilize and bind to AgNPs through their anionic part. DFT calculations have been undertaken to understand the stabilization mechanism better. The optimized geometry arrived through these calculations also shows that the model 13 atom Ag cluster interacts with IL molecules through their anionic portions. Negative value of binding energy and interaction energy indicates the higher stability of synthesized NPs. The calculated IR spectrum supports this conclusion. Moreover, the large HOMO-LUMO gap of the pure IL decreases significantly for the model Ag13-IL entity. Therefore, the DFT calculations predict that the prepared material has a visible range band gap and could have important photocatalytic applications.

Declarations

Author contribution statement

Madhulata Shukla: Performed the experiments; Wrote the paper.

Alkadevi Verma: Analyzed and interpreted the data.

Sunil Kumar, Shaili Pal: Contributed reagents, materials, analysis tools or data.

Indrajit Sinha: Conceived and designed the experiments; Wrote the paper.

Funding statement

This work was supported by UGC, India (F.30-446/2018 (BSR)).

Data availability statement

Data included in article/supplementary material/referenced in article.

Declaration of interests statement

The authors declare no conflict of interest.

Additional information

Supplementary content related to this article has been published online at https://doi.org/10.1016/j.heliyon.2021.e06065.

Acknowledgements

IIT-BHU acknowledged for providing computational facilities.

References

[1] J. Dupont, J.D. Scholten, On the structural and surface properties of transition-metal nanoparticles in ionic liquids, Chem. Soc. Rev. 39 (2010) 1780–1804.
[2] J.D. Scholten, B.C. Leal, J. Dupont, Transition metal nanoparticle catalysis in ionic liquids, ACS Catal. 2 (2012) 184–200.
[3] S. Wegner, C. Janiak, Metal nanoparticles in ionic liquids ionic liquids II, Top. Curr. Chem. (2017) 153–184.
[4] A. Podgorsek, A.S. Pensado, C.C. Santini, M.F. Costa Gomes, A.A.H. Padua, Interaction energies of ionic liquids with metallic nanoparticles: solvation and stabilization effects, J. Phys. Chem. C 117 (2013) 3537–3547.
[5] M. Shukla, I. Sinha, Catalytic activation of nitrobenzene on PVP passivated silver cluster: a DFT investigation, Int. J. Quant. Chem. (2018) e25490.
[6] E. Redel, R. Thomann, C. Janiak, First correlation of nanoparticle size-dependent formation with the ionic liquid anion molecular volume, Inorg. Chem. 47 (2008) 14–16.
[7] C.M. Correa, M.A. Bizeto, F.F. Camilo, Direct synthesis of silver nanoparticles in ionic liquid, J. Nanopart. Res. 18 (2016) 132.
[8] J. Dupont, P.A.Z. Suarez, Physico-chemical processes in imidazolium ionic liquids, Phys. Chem. Chem. Phys. 8 (2006), 2441-2252.
[9] L.L. Lazarus, C.T. Riche, N. Malmstadt, R.L. Brutchey, Effect of ionic liquid impurities on the synthesis of silver nanoparticles, Langmuir 28 (2012) 15987–15993.
[10] Z. He, P. Alexandridis, Nanoparticles in ionic liquids: interactions and organization, Phys. Chem. Chem. Phys. (2015).
[11] T.A. Kareem, A.A. Kaliani, ZnS nanoparticle synthesis in 1-butyl-3-methylimidazolium tetrafluoroborate by simple heating, Arab. J. Chem. 12 (2019) 2810–2816.
[12] S. Suzuki, Y. Tomita, S. Kuwabata, T. Torimoto, Synthesis of alloy AuCu nanoparticles with the L10 structure in an ionic liquid using sputter deposition, Dalton Trans. 44 (2015) 4186–4194.
[13] E.E. Zvereva, S.A. Katsyuba, P.J. Dyson, A.V. Aleksandrov, Solvation of palladium clusters in an ionic liquid: a QM/MM molecular dynamics study, J. Phys. Chem. C 120 (2016) 4596–4604.
[14] H. Abroshan, Li Gao, Jizhi Lin, Hyung J. Kim, Rongchao Jin, Molecular mechanism for the activation of Au25(SCH2CH2Ph)18 nanoclusters by imidazolium-based ionic liquids for catalysis, J. Catal. 337 (2016) 72–79.
[15] A.I. Bhatt, A. Mechler, L.L. Martin, A.M. Bond, Synthesis of Ag and Au nanostructures in an ionic liquid: thermodynamic and kinetic effects underlying nanoparticle, clusters and nanowire, J. Mater. Chem. 17 (2007) 1–12.
[16] M. Okumura, Y. Kitagawa, T. Kawakami, M. Haruta, Theoretical investigation of the hetero-junction effect in PVP-stabilized Au_{13} clusters. The role of PVP in their catalytic activities, Chem. Phys. Lett. 459 (2008) 133–136.
[17] A.M. Abdelghany, M. Sh. Mekhail, E.M. Abdelrazek, M.M. Aboud, Combined DFT/FTIR structural studies of monodispersed PVP/Gold and silver nano particles, J. Alloys Compd. 646 (2015) 326–332.
[18] R. Devasenathipathy, Y.X. Liu, C. Yang, K.K. Rani, S.F. Wang, Simple electrochemical growth of copper nanoparticles decorated silver nanoleaves for the sensitive determination of hydrogen peroxide in clinical lens cleaning solutions, Sensor. Actuator. B 252 (2017) 862–869.
[19] A. Verma, R.K. Gupta, M. Shukla, M. Malviya, I. Sinha, Ag–Cu bimetallic nanoparticles as efficient oxygen reduction reaction electrocatalysts in alkaline media, J. Nanosci. Nanotechnol. 20 (2020) 3.
[20] A. Verma, M. Shukla, S. Kumar, S. Pal, I. Sinha, Mechanism of visible light enhanced catalysis over curcumin functionalized Ag nanocatalysts, Spectrochemica Acta-A Mol. Biomol. Spectrosc. (2020).
[21] M.J. Frisch, G.W. Trucks, H.B. Schlegel, G.E. Scuseria, M.A. Robb, J.R. Cheeseman, G. Scalmani, V. Barone, G.A. Petersson, H. Nakatsuji, X. Li, M. Caricato, A.V. Marenich, J. Bloino, B.G. Janesko, R. Gomperts, B. Mennucci, H.P. Hratchian, J.V. Ortiz, A.F. Izmaylov, J.L. Sonnenberg, D. Williams-Young, F. Ding, F. Lipparini, F. Egidi, J. Goings, B. Peng, A. Petrone, T. Henderson, D. Ranasinghe, V.G. Zakrzewski, J. Gao, N. Rega, G. Zheng, W. Liang, M. Hada, M. Ehara, K. Toyota, R. Fukuda, J. Hasegawa, M. Ishida, T. Nakajima, Y. Honda, O. Kitao, H. Nakai, T. Vreven, K. Throssell, J.A. Montgomery Jr., J.E. Peralta, F. Ogliaro, M.J. Bearpark, J.J. Heyd, E.N. Brothers, K.N. Kudin, V.N. Staroverov, T.A. Keith, R. Kobayashi, J. Normand, K. Raghavachari, A.P. Rendell, J.C. Burant, S.S. Iyengar, J. Tomasi, M. Cossi, J.M. Millam, M. Klene, C. Adamo, R. Cammi, J.W. Ochterski, R.L. Martin, K. Morokuma, O. Farkas, J.B. Foresman, D.J. Fox, Gaussian, Inc., 2016. Wallingford CT.
[22] A.D. Becke, Density-functional thermochemistry. III. The role of exact exchange, J. Chem. Phys. 98 (1993) 5648–5652.
[23] C. Lee, W. Yang, R.G. Parr, Development of the Colle-Salvetti correlation-energy formula into a functional of the electron density, Phys. Rev. B 37 (1988) 785–789.
[24] P.J. Hay, W.R. Wadt, *Ab initio* effective core potentials for molecular calculations. Potentials for the transition metal atoms Sc to Hg, J. Chem. Phys. 82 (1985) 270–283.
[25] N.M. O'Boyle, GaussSum, Version 2.0.5, 2007. Available at, http://gausssum.sf.net.
[26] F. Samari, S. Dorostkar, Synthesis of highly stable silver nanoparticles using imidazolium-based ionic liquid, J. Iran. Chem. Soc. 13 (2016) 689–693.
[27] J.B. Chang, C.H. Liu, J. Liu, Y.Y. Zhou, X. Gao, S.D. Wang, Green-chemistry compatible approach to TiO_2-supported PdAu bimetallic nanoparticles for solvent-free 1-phenylethanol oxidation under mild conditions, Nano-Micro Lett. 7 (2015) 307–315.
[28] E. Redel, M. Walter, R. Thomann, C. Vollmer, L. Hussein, H. Scherer, M. Krger, C. Janiak, Synthesis, stabilization, functionalization and, DFT calculations of gold nanoparticles in fluorous phases (PTFE and ionic liquids), Chem. Eur J. 15 (2009) 10047–10059.
[29] C. Janiak, Review ionic liquids for the synthesis and stabilization of metal nanoparticles, Z. Naturforsch 68b (2013) 1059–1089.
[30] P. Cheng, C. Liu, Y. Yang, S. Huang, First-principle investigation of the interactions between Pt_xRu_{55-x} ($x = 0$, 13, 42, 55) nanoparticles and [BMIM][PF_6] ionic liquid, Chem. Phys. 452 (2015) 1–8.
[31] E.A. Turner, C.C. Pye, R.D. Singer, Use of ab-initio calculation towards the rational design of room temperature ionic liquids, J. Phys. Chem. A 107 (2003) 2277e2288.